Indian Journal of Fibre & Textile Research
Vol. 44, September 2019, pp. 338-343

Modelling and simulation of 3D orthogonal and interlock fabrics for structural composite applications

Ashwini Kumar Dash & Bijoya Kumar Behera[a]
Department of Textile Technology, Indian Institute of Technology Delhi, New Delhi 110 016, India

Received 31 January 2018; revised received and accepted 20 June 2018

Modelling and simulation of 3D orthogonal and interlock fabrics have been studied for tensile applications. This involves building a geometrical model by calculating the proper dimensions of the tows, conversion of the geometrical model into finite element mesh, and subsequently, prediction of tensile properties in the direction of load bearing tows by simulation using meso-finite element modelling. For the simulation, elliptical tow cross-section with aspect ratio 11 has been preferred as the best geometrical modelling parameter. Model results obtained from finite element analysis are then compared with experimental values to authenticate the modelling methodologies. The simulated results of maximum stress at break are found to be higher than the experimental results for both the corresponding orthogonal and interlock structures.

Keywords: Composite, 3-Dimensional reinforcement, 3D orthogonal fabric, Finite element method, Interlock fabric, Modelling, Stress-strain analysis

1 Introduction

Composites manufactured using textile fabrics as reinforcement draw more attention because of their high stiffness, strength to weight ratio, good fatigue strength, excellent corrosion resistance, and good dimensional stability. In addition to the above benefits, larger volumes of the textile reinforced composites can be produced at a faster rate with minimum fabrication cost as well as cycle time. Among all fabric manufacturing techniques weaving is the most prevailing method for the preparation of reinforcements because it offers excellent balance between warp and weft yarns and has superior cover in comparison to other methods of fabric production. 2D fabrics using high performance yarns as reinforcement are well established in structural composite fields[1-6]. However, most of the 2D reinforcements lead to inferior out of plane mechanical properties when used as a composite[7,8]. Three dimensional (3D) fabrics came into the picture for their integrated structure with a yarn in through-thickness direction[9]. These 3D fabrics can be produced into near net shape so that the overall fabrication cost can be reduced for a particular end use.

The mechanical properties of the 3D fabrics can be ascertained through their experimental characterization, which is a costly method. Many researchers[10-12] attempted on various predicting modelling approach, which is an inexpensive alternative. Most of the researchers worked on modelling of textile materials at the level of unit cell at mesostructural level[13-14].

This paper enumerates modelling of basic 3D solid structures (orthogonal and interlock fabrics) and proposes a road map at the mesostructural level – the level of a unit cell (representative volume element, repeat) of the material structure. The corresponding algorithms are (i) finding the unit cells and analyzing the mechanical properties of the unit cell using FEM; and (ii) regenerating the entire geometry by assembling the unit cells for predicting stress-strain characteristics of the reinforcement as a whole. Model results obtained from finite element analysis are compared with experimental values to authenticate the modelling methodologies as well modelling results.

2 Materials and Methods

2.1 Materials

For the preparation of fabric samples, E-glass tows of 1200, 600 and 300 tex were used for stuffers, fillers, and binders respectively. The measured tenacity and initial modulus of the E-glass tows were 5.78 g/den (CV % 5.95) and 233 g/den (CV % 2.92) respectively.

2.2 Weaving of Fabric Samples

The fabrics were produced in a sample weaving machine with some modification to attach an extra

[a]Corresponding author.
E-mail: behera@textile.iitd.ac.in

Table 1 — Weaving details of orthogonal and interlock fabrics

Weave	N_s	N_f	N_b	Reed count	Denting	EPM stuffer/ layer	EPM binder	EPM filler/layer	Width of the fabric, m
Orthogonal	1200	600	300	20	3S/B1/3S/B2	198	198	315	0.46
Interlock	1200	600	300	20	3S/B1/3S/B2/3S/B3/3S/B4/3S/B5	198	198	315	0.46

N_s, N_f, N_b — Stuffer, filler, and binder linear densities respectively. EPM — ends per metre. 3S indicates 3 stuffers/dent and B1, B2…, B5 indicate different binders/dent.

beam for binder tows with separate let off arrangements. The weaving parameters are given in Table 1.

2.3 Tensile Testing of Fabric Samples

Zwick/Roell universal testing machine using 50 kN load-cell was used to carry out tensile tests of five different samples from each fabric according to ASTM-D 5035. The measured thickness and GSM of the orthogonal fabrics were 1.68 mm (CV% 1.66) and 1617 g/m^2 (CV% 0.80) respectively and that of interlock fabrics were 1.62 mm (CV% 4.09) and 1675 g/m^2 (CV% 0.30) respectively.

2.4 Theoretical Consideration

2.4.1 Modelling in Solidworks

Solidworks is a solid modeler and utilizes a parametric feature-based approach to create models and assemblies. Parameters in terms of values are applied to form the shape as well as geometry of the models and assemblies. Parameters are of two types, viz numeric, and geometric. Features are generally used for building blocks. It can be achieved by either shape based or operation based approach. Building of a model initiates with 2D or 3D sketch and subsequently, those are extruded or cut to achieve the solid design. Operation based feature approach involves the use of fillets, chamfers, and shells.

The parametric nature of Solidworks ensures building of the geometry from the dimensions of different parameters and their inter relations. Mating is done while assembling the parts by the selection of proper planes of different parts. Sketch relations involve parallelism, tangency, concentricity, etc. Assembly relations include parts and components. Models can be done either solely in part or in assembled form.

2.4.1.1 Calculation of Geometric Parameters for Modelling

Geometrical modelling of 3D woven solid structures [15, 16] reveals that the experimental values of areal density, thickness and fibre volume fractions of the fabric are quite close to the values obtained from modelling approach when elliptical cross-section with aspect ratio (AR) of 11 was taken into account. Hence in this study, these parameters were considered for modelling the unit structure. Tow linear densities of 1200, 600 and 300 tex were used for stuffer, filler, and binders respectively. The thicknesses of the stuffer, filler, and binder tows were calculated from their linear density, assumed packing factor and aspect ratio, as per the following equation:

Table 2 — Length of major and minor axes of elliptical tows of different linear densities

Tow linear density tex	Length, mm	
	Major axis	Minor axis
1200	2.904	0.264
600	2.057	0.187
300	1.452	0.132

$$h_i = 2\sqrt{\frac{\mu_i}{\rho(AR)P\pi}} \text{(stuffer, filler, and binder)} \quad \ldots (1)$$

where μ_i is the linear density of stuffer, filler and binder; ρ, the density of stuffer, filler, and binder tows; and AR, the aspect ratio. The filaments within the tow were assumed to be circular and not 100% packed together. Therefore, a tow-packing factor (P) was incorporated i.e. $P = \pi/4 \approx 0.7854$ (for rectangular packing array). Using Eq. (1), the minor axes of the tows (thicknesses) were calculated. The length of the major axes was calculated using aspect ratio of the tows, i.e. 11. The major and minor axes parameters of different tows are given in Table 2.

2.4.1.2 Generation of Unit Cell

The tows were assumed as isotropic monofilaments to facilitate simple model with least possible number of nodes as well as number of elements in the structures. The unit cell models of the orthogonal and interlock structures generated in Solidworks 2014 are shown in Fig. 1.

These models have three layers of stuffer tows, four layers of filler tows for both the structures. The number of binder tows was two and five for the orthogonal and interlock structures respectively.

2.4.2 Finite Element Method (FEM)

Finite element method, very often referred to as finite element analysis, is a numerical analysis tool which is used to solve various engineering and mathematical problems. This method resolves various problems relating to heat transfer, mass transport, fluid flow, and

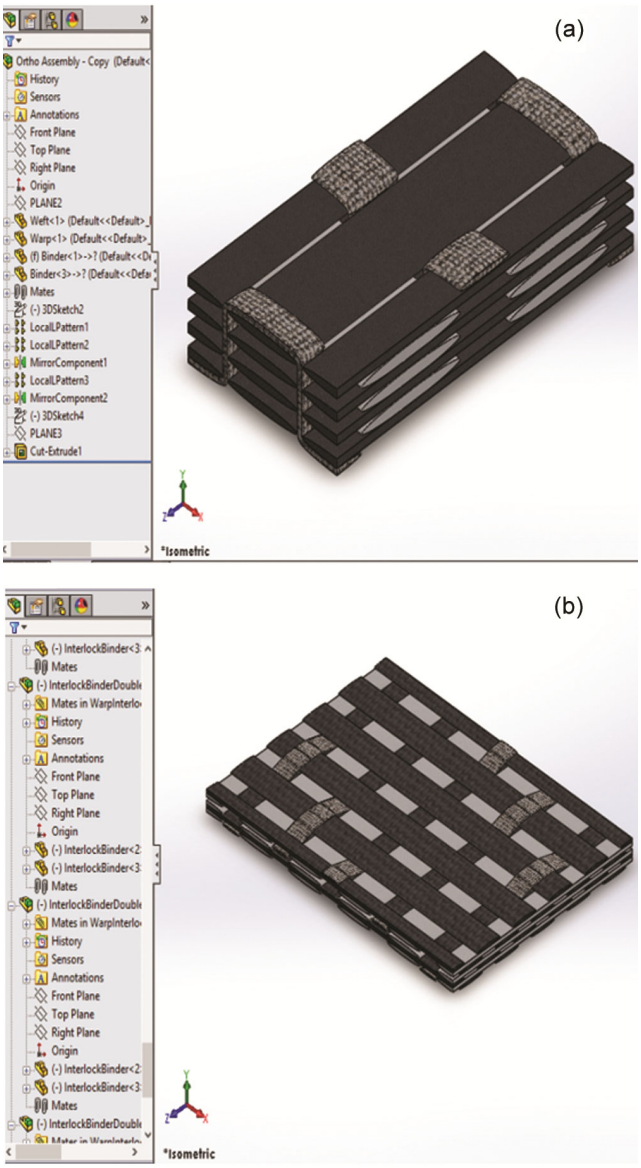

Fig. 1 — Unit cell models generated in Solidworks 2014 (a) Orthogonal and (b) Interlock

structural analysis. It leads to a comparative solution to partial differential equations as well as integral equations. It gives approximate values to the unknowns at distinct number of points at the domain through a system of algebraic equations. Bigger elements are divided into various smaller elements which are termed as finite elements. Smaller equations are exercised to configure bigger system of equations. FEM then uses variation methods from the calculus of variations to a closer solution by minimizing an associated error function.

2.4.3 Ansys

Ansys is an American computer-aided engineering software (Pennsylvania, USA). Ansys publishes engineering analysis software across a range of disciplines including FEM, structural analysis, computational fluid dynamics, explicit and implicit methods, and heat transfer. It is available as Ansys Autodyn, Ansys mechanical, Ansys fluid dynamics, and Ansys electronics commercially. Ansys mechanical includes finite element analysis tool for structural analysis as well as thermal analysis.

In this study, structural analysis mode was used, which basically deals with linear, nonlinear, and dynamic studies. The models developed in Solidworks were imported to the Ansys workbench and simulation was carried out with the following procedures.

2.4.3.1 Import of Unit Cell

The models thus created in Solidworks were imported to Ansys workbench. The dimension of the unit cell of orthogonal as well as interlock structures thus calculated were 4.378 mm (length) × 8.712 mm (width) ×1.825 mm (height) and 31.750 mm (length) × 21.780 mm (width) × 1.804 mm (height) respectively. The volume and mass of the orthogonal unit cell was 3.9058×10^{-8} m^3 and 3.0661×10^{-4} kg and that of interlock unit cell was 2.8749×10^{-7} m^3 and 7.3023×10^{-4} kg respectively. The effective number of stuffer, filler, and binder tow were 6, 8, and 2 respectively for orthogonal structure and 15, 20 and 5 respectively for interlock structure. The stuffers/m as well as binders/m were 198 and fillers/m was 315 for both the orthogonal and interlock fabrics.

Assignment of Material Properties

The material properties of E-glass were assigned to each parts of the models, such as Young's modulus 67,170 MPa (tested as per ASTM E111-04), density of material 2540 kg/m^3 (tested as per ASTM C693-93), coefficient of inter yarn friction 0.3 (tested as per ASTM 3412), tensile yield strength 1538 MPa (tested as per ASTM D2343), tensile ultimate strength 3100 MPa (tested as per ASTM D2343) and Poisson's ratio 0.22 (tested as per ASTM E132-04).

2.4.3.2 Mesh Formation

For the analysis purpose, bigger elements were converted into smaller finite elements. The element shape was chosen by the fine automatic mesh generator. Mesh generation is shown in Fig. 2.

Mesh statistics constitute 21 active bodies, 136234 nodes and 26173 elements for orthogonal unit cell and 50 active bodies, 154070 nodes and 24534 elements for interlock unit cell. Nodes and elements generated by Ansys meshing commands use the global Cartesian coordinate system and active element coordinate system respectively.

2.4.3.3 Boundary Conditions

Fixed Support

Fixed support was given to one of the planes in the stuffer direction to facilitate loading in the opposite direction.

Frictionless Support

Frictionless support was given to avoid distortion of the unit cell during loading. This ensures that there will be no exaggeration of the model in the direction perpendicular to the surface. This was applied in all faces except fixed support face and load application face.

Application of Load

Finite element loads are independent of the mesh configuration. Mesh elements are changeable while the applied loads remain unaffected. Thus, mesh modification and mess sensitivity studies are possible without the application of loads at each instance. Thus, distinguishable coordinate systems and preferred loading directions can be ascertained by finite element analysis.

In this study, tensile load is applied along the stuffer direction which is the main load bearing tow in real applications. Pressure load is preferred to that of point load so that uniform force can be distributed on the surface of the stuffer yarn[17] [Figs 3 (a) and (b)] and is applied on the opposite direction of the fixed support.

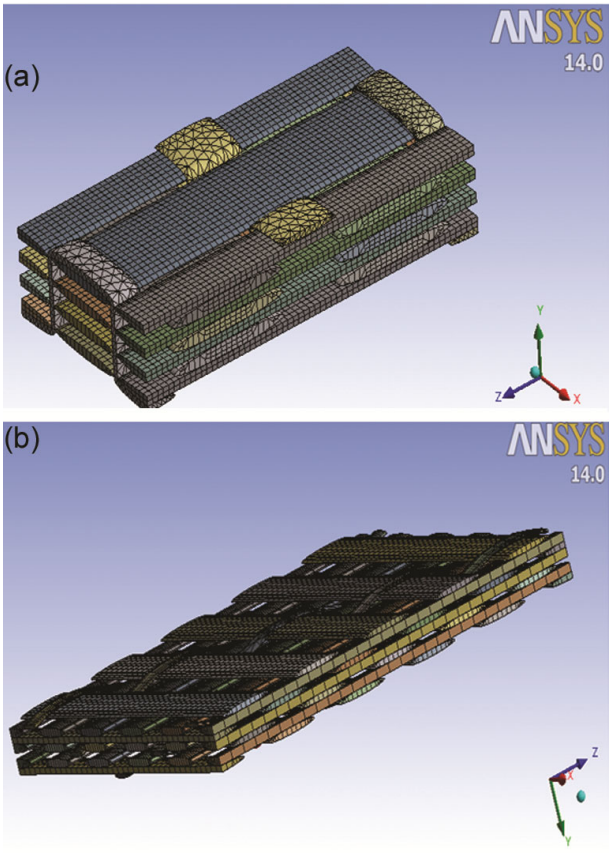

Fig. 2 — Mesh generation on the unit cells (a) orthogonal and (b) interlock

3 Results and Discussion

The simulated results of maximum stress and strain are obtained in the direction of stuffers for both the orthogonal and interlock structures. Experimentally the stress-strain curve of one example of specimens of the two structures has been plotted, with stress and strain recorded until failure.

3.1 Simulated and Experimental Results of Orthogonal Structure

The simulated image for one particular pressure load is shown in Fig. 4. The simulated results of maximum

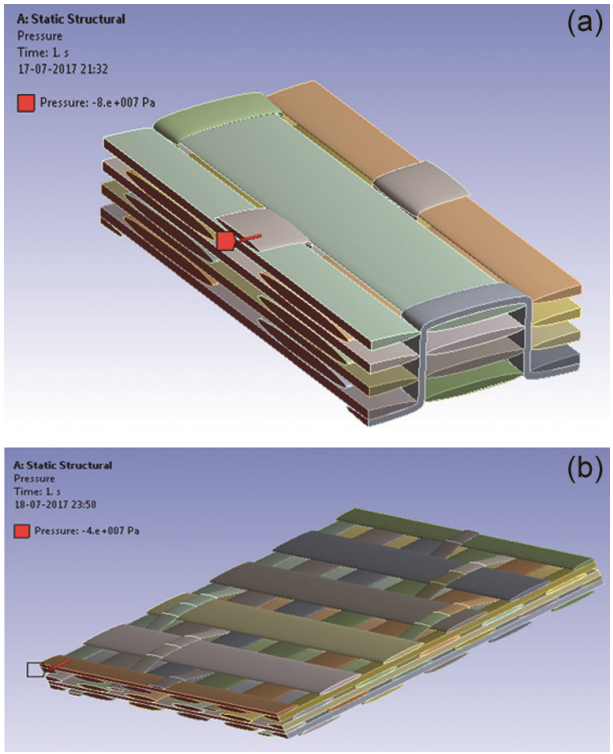

Fig. 3 — Pressure load applied in stuffer direction (a) orthogonal and (b) interlock

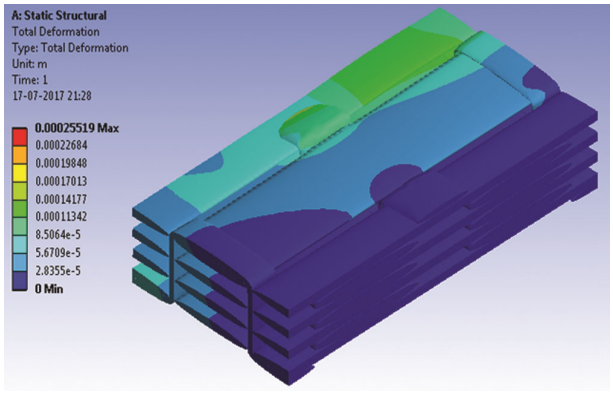

Fig. 4 — Simulated image showing total deformation of orthogonal structure at a particular pressure.

stress at different pressure levels are given in Table 3. Similarly, with the applied pressure, strain rate has been obtained and the results are shown in Table 3.

The stress-strain behavior obtained from FEM simulation and experimental results are given in Figs 5 (a) and (b), which show that the relation is almost linear.

Table 3 — Simulated results of maximum stress and strain rate for orthogonal structure

Pressure applied, MPa	Maximum stress, MPa	Strain
10	1.11	0.002
20	10.25	0.009
40	19.58	0.017
60	38.52	0.034
80	69.56	0.058
120	100.25	0.082
200	156.25	0.128

Table 4 — Simulated results of maximum stress and strain rate for interlock structure

Pressure applied, MPa	Maximum stress, MPa	Maximum strain
10	4.25	0.005
20	8.19	0.01
40	15.12	0.02
60	30.23	0.037
80	55.56	0.06
120	89.56	0.085
200	129.69	0.11
400	180.62	0.14

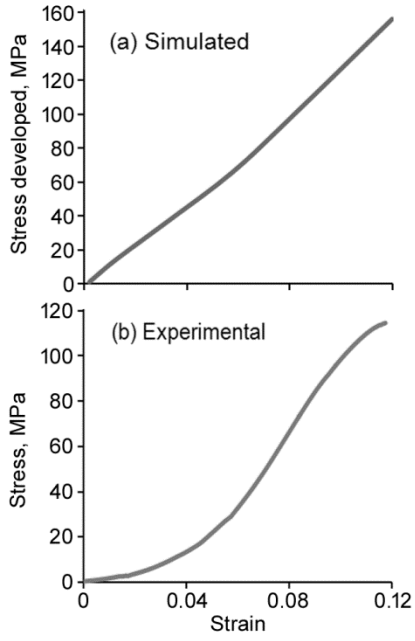

Fig. 5 — Simulated and experimental stress-strain curve of orthogonal sample

From the above figure, it is observed that the average breaking stress is 114.3 MPa at strain % of 11.73. But the simulated stress at this level of strain is noted to be higher. A similar study is undertaken for orthogonal fabrics using race track cross-sections of constituent tows and it shows the same trend[17].

3.2 Simulated and Experimental Results of Interlock Structure

The stress distribution and total deformation for one particular pressure load is shown in Fig. 6. The simulated results of maximum stress and strain rate at different pressure levels are shown in Table 4.

The stress-strain behavior obtained from FEM simulation is given in Fig. 7(a), which shows that the relation is more or less linear and trend is mostly

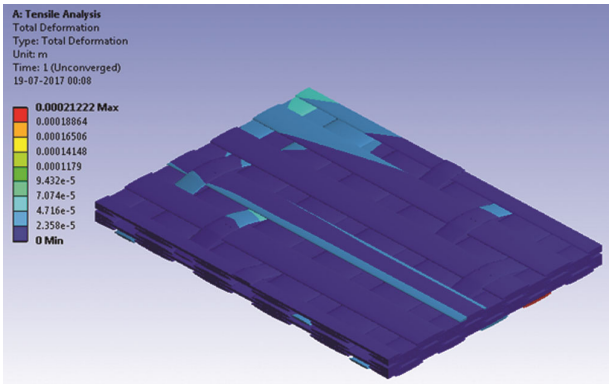

Fig. 6 — Simulated image showing total deformation of interlock structure at a particular pressure

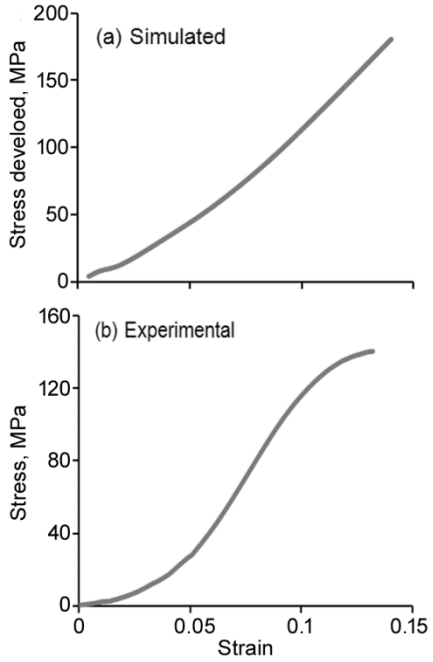

Fig. 7 — Simulated and experimental stress-strain curve of interlock sample

similar with that of orthogonal structure. The stress-strain curve obtained from the experiment is shown in Fig. 7(b).

From the above figures, it can be observed that the average breaking stress is 140.1 MPa at strain % of 13.18. But the simulated stress at this level of strain is observed to be higher. This observation is approximately similar to that of orthogonal structure as discussed earlier.

4 Conclusion

Finite element analysis is a powerful tool to predict the mechanical properties of the textile reinforced composites. Textile structures do have some peculiar characteristics for which these methods need to have some deeper insight. In reality, the filler tows have some amount of crimp due to the movement of binder tows. Also it is obvious that the binder tows never follow the idealized path as shown in the model. This leads the micro structure of 3D fabrics very complex for analysis using this software. Further, the mechanical properties are regulated by numerous parameters, thus it becomes challenging to have a proper validation. These models have only included major architectural parameters to demonstrate the state of stress and failure mode and hence fails at micro structural level. These need to be further improved incorporating the waviness of the tows as one of the major architectural parameters and then experimentally validated. A reliable database can be established with predicted results which will be helpful for practical design and production of textile based composites.

References

1 Ishikawa T & Chou T W, *J Compos Mater,* 16 (1982) 2.
2 Ishikawa T & Chou T W, *J Mater Sci,* 17 (1982) 3211.
3 Wang Y, Gowayed Y, Kong X, Li J & Zhao D, *J Compos Technol Res,* 17 (1995) 283.
4 Ramasamy A,Wang Y & Muzzy J, *Polym, Compos,* 17 (1996) 515.
5 Shembekar P S & Naik N K, *J Compos Mater,* 26 (1992) 2226.
6 Wang Y & Zhao D, *Composites*, 26 (1995) 115.
7 Clarke S, *Soc Adv Mater Process Eng J (SAMPE)*, 34 (1998) 35.
8 Stobbe D & Mohamed M, *Cost and performance viability* in *commercial applications,* paper presented at the 48th International SAMPE symposium, Long Beach, CA, 11-15 May 2003.
9 Chen X , Taylor L W & Tsai L J, *Text Res J,* 81 (2011) 932.
10 Ansar M, Xinwei W & Chouwei Z, *Compos Struct,* 93 (2011) 1947.
11 Lomov S V, Huysmans G, Luo Y, Parnas R S, Prodromou A, Verpoest I & Phelan F R, *Compos [Part A] Appl Sci Manuf,* 32 (2001) 1379.
12 Tan P, Tong L & Steven G, *Compos [Part A] Appl Sci Manuf,* 28 (1997) 903.
13 Lomov S V, Gusakov A V, Huysmans G, Prodromou A & Verpoest I, *Compos Sci Technol,* 60 (2000) 2083.
14 Lomov S V, Huysmans G & Verpoest I, *Text Res J,* 71 (2001) 534.
15 Buchanan S, Grigorash A, Quinn J P, McIlhagger A T & Young C, *J Text Inst,* 101 (2010) 679.
16 Dash B P, Behera B K , Mishra R & Militky J, *J Text Inst,* 104 (2013) 312.
17 Mishra R , Militky J , Behera B K & Banthia V, *J Text Inst,* 103 (2012) 1255.